GEOPHYSICAL RESEARCH LETTERS, VOL. 35, L13805, doi:10.1029/2008GL033918, 2008

On the correlation between ice water content and ice crystal size and its application to radiative transfer and general circulation models

K. N. Liou,[1] Y. Gu,[1] Q. Yue,[1] and G. McFarguhar[2]

Received 19 March 2008; revised 15 May 2008; accepted 2 June 2008; published 4 July 2008.

[1] We performed correlation analysis involving ice water content (*IWC*) and mean effective ice crystal size (*De*) intended for application to climate models. For this purpose, ice crystal size distributions obtained from in situ measurements conducted from numerous field campaigns in the tropics, midlatitude, and Arctic regions were used and we show that *IWC* and *De* are well-correlated in this regional division. Including temperature classification in midlatitude cases increases this correlation. We applied the correlation results to cloud radiative forcing calculations in terms of *IWC*, in which *De* is expressed as a baseline mean and deviation from uncertainty in small ice crystal measurements. The latter deviates from the mean by less than 2 W/m^2 in net radiative forcing. Using the correlation results, simulations from the UCLA GCM showed substantial regional deviations in OLR and precipitation patterns from assuming a constant *De*. **Citation:** Liou, K. N., Y. Gu, Q. Yue, and G. McFarguhar (2008), On the correlation between ice water content and ice crystal size and its application to radiative transfer and general circulation models, *Geophys. Res. Lett.*, *35*, L13805, doi:10.1029/2008GL033918.

1. Introduction

[2] In recent years, development in cloud modeling has included prognostic equations for the prediction of *IWC* for high-level clouds formed in GCMs and climate models. This is a milestone accomplishment from the standpoint of incorporating a physically-based cloud microphysics scheme in these models, and at the same time, it is also essential from the perspective of studying cloud-radiation interactions. However, cloud particle size is also an independent parameter that affects radiation transfer. For example, for a given *IWC* in clouds, smaller particles would reflect more sunlight than larger counterparts, an effect that has been recognized by *Twomey et al.* [1984] and *Liou and Ou* [1989] in conjunction with aerosol-cloud indirect effects. Ice crystal size and shape in the Earth's atmosphere are complex and intricate. After initial homogeneous and/or heterogeneous nucleation involving suitable aerosol particles and atmospheric conditions, ice crystal growth is governed by diffusion processes and subsequent actions by means of collision and coalescence. These physical processes are complicated by the nature of the ice crystal's hexagonal and irregular shape. Incorporating a fully interactive ice microphysics based on the first principle in a GCM appears to be a challenging but an extremely difficult computational task. Innovative *De* parameterization based on theory and observation must be developed for GCM applications.

[3] It has been a common practice to prescribe a mean effective ice crystal size in GCMs [see, e.g., *Gu et al.*, 2003]. A number of GCMs has also used temperature to determine *De* [*Kristjánsson et al.*, 2005; *Gu and Liou*, 2006]. This approach is rooted in earlier ice microphysics observations from aircraft, and attests to the fact that small and large ice crystals are related to cold and warm temperatures in cirrus cloud layers. *Ou and Liou* [1995] developed a parameterization equation relating cirrus temperature to a mean effective ice crystal size based on a large number of midlatitude cirrus microphysics data presented by *Heymsfield and Platt* [1984]. *Ou et al.* [1995] reduced large standard deviations in the size-temperature parameterization by incorporating a dimensional analysis between *IWC* and *De*. Using CEPEX data, *McFarquhar et al.* [2003] developed a *De* parameterization as a function of *IWC* for use in a single column model.

[4] This short paper illustrates that *De* has a high correlation with *IWC* based on theoretical consideration and regional observational data analysis, and that this correlation can be effectively parameterized for use in a GCM setting for interactive cloud-radiation analysis. We report on an analysis of substantial ice microphysics datasets available from a number of field campaigns and determine the statistical correlation between *De* and *IWC*, followed by a discussion on application of the *De-IWC* correlation to an offline radiative transfer calculation and a GCM simulation.

2. Analysis of Ice Microphysics Data

[5] In the correlation analysis, we divided available datasets in accordance with three geographical areas (tropics, midlatitude, and Arctic) because of their distinct ice cloud formation processes. A significant fraction of tropical cirrus are generated from towering cumulus convection, but the majority of midlatitude cirrus clouds are primarily related to large-scale frontal and synoptic systems and mesoscale topographical forcings. In Arctic regions, the formation of ice clouds appears to be directly related to cold temperature, large-scale transport of sensible and latent heat, and boundary layer turbulence. We should first introduce ice water content defined by

$$IWC = \int V(L)\rho_i n(L)dL,$$

[1]Department of Atmospheric and Oceanic Sciences and Joint Institute for Regional Earth System Science and Engineering, University of California, Los Angeles, California, USA.

[2]Department of Atmospheric Sciences, University of Illinois, Urbana, Illinois, USA.

0094-8276/08/2008GL033918$05.00

where $n(L)$, the ice crystal size distribution, is unknown in current GCMs; $V(L)$ is the volume of an individual ice crystal that accounts for shape factor; ρ_i is the density of ice; and L is the ice crystal maximum dimension. We may define a mean effective ice crystal size in the form

$$De = \int V(L)n(L)dL / \int A(L)n(L)dL = IWC / \left[\rho_i \int A(L)n(L)dL\right] = IWC/\rho_i Ac,$$

where $A(L)$ is the cross-sectional area for an individual ice crystal and A_c represents the total projected area for a given ice crystal size and habit distribution. *Heymsfield and McFarquhar* [1996] found that $A_c \sim$ a IWC^b where a and b are empirical coefficients. The A_c-*IWC* relation further illustrates a direct correlation between *De* and *IWC*. Larger (smaller) *IWCs* imply larger (smaller) *Des,* which is in line with the ice crystal growth by means of diffusion and accretion. The definition of this mean effective size effectively accounts for ice crystal size and shape distributions in light scattering calculations [*Fu and Liou*, 1993; *Yang et al.*, 2000]. However, their relationship is not unique but is constrained by A_c. We followed the procedures developed by *Yue et al.* [2007] and *Yang et al.* [2000, 2005] for *IWC*, *De*, and A_c calculations required in correlation development.

[6] Uncertainty in the measurement of small ice crystals <100 μm from aircraft platforms has been an important issue in scientific discussion. Shattering of millimeter-sized ice particles in collision with the probe can artificially enhance the concentration of small ice crystals [e.g., *Heymsfield et al.*, 2006]. Some researchers [e.g., *Boudala et al.*, 2002] suggested that the FSSP instrument may give a reasonable estimate of small ice particles. Because of the uncertainty in small ice crystal measurements, we have conducted three independent *IWC-De* correlation experiments: (1) maximizing small ice crystals; (2) reducing concentration of these smaller ice crystals (N_{sm}) by one order of magnitude; and (3) reducing N_{sm} by two orders of magnitude. Experiment 2 is used as the base run, while the other two give a possible range of parameterized De due to uncertainties in small ice crystal measurements.

[7] (a) For tropical cases, a total of 40469 in situ measurements of ice crystal size distribution (SD) were available for analysis including 5460 from CRYSTAL-FACE, and 35009 from CEPEX. The former data were collected by CAPS on board NASA's WB57 on nine different dates in July 2002. CEPEX data included measurements from a 2-DC probe for ice crystals larger than about 100 μm and a parameterization for N_{sm} based on VIPS measurements [*McFarquhar and Heymsfield*, 1997] in March and April, 1993. These instruments were on board Aeromet Learjet. Both the original CEPEX and PARTICLE-FACE datasets were composed of ice crystal measurements averaged in 30 s intervals. Due to the low sampling rate of CRYSTAL-FACE data, SDs from this experiment were averaged over 5 min. We selected datasets having more than 5-channel size measurements to ensure proper size average. As a result, only 261 CRYSTAL-FACE and 11032 CEPEX cases were used in the correlation study. From the analysis of CEPEX data, about 34 and 66 % of ice crystals are solid columns and bullet rosettes/aggregates, respectively. The effect of ice crystal habit on *De* parameterization is an intricate subject requiring further in-depth study.

[8] Figure 1a displays 11293 data points in a 2D logarithmic domain. The *IWC* values span from 10^{-6} to ~ 1 g/m^3, while *De* ranges from $\sim 20-200$ μm. We used the χ^2 best fit to these observed data to obtain the best parameterization equation in polynomial as follows:

$$\ln(De) = \mathrm{a} + \mathrm{b}\ \ln(IWC) + \mathrm{c}(\ln(IWC))^2,$$

where a = 5.4199, b = 0.35211, and c = 0.012680. Uncertainty in N_{sm} can result in deviations from the base run from 5% to 40%, as *IWC* decreases, much large than the standard deviation from statistical uncertainty. We also attempted to correlate *De* and in situ temperature measurements ($-70 - -20$°C), but the 2D data points are extremely scattered without a consistent pattern. In this case, temperature is not a suitable variable for *De* determination, probably due to the predominant convective nature of cloud systems in the tropics such that vertical velocity is a more important parameter in regulating *De*.

[9] (b) A total of 4033 in situ size distribution measurements were obtained for midlatitute cases taken at the ARM SGP site. Ice crystals larger than 100 μm were measured by 2D-C probe on board the UND Citation. SD was extrapolated to 2 μm using the parameterization developed by *Ivanova et al.* [2001] using FSSP measurements obtained in an ARM experiment. Aircraft datasets were composed of measurements averaged at 5 s intervals. Only the SDs that had measurements greater than 5-size channels were selected, resulting in only 3919 cases. *IWC* ranges from $\sim 10^{-4}$–10^{-1} g/m^3, while *De* has values from $\sim 30-140$ μm. Although habit information from ARM data sources was not available, previous studies revealed that for midlatitude cirrus clouds, ice crystal shape spans from bullet rosettes and aggregates (60%) to hollow columns (20%) to plates (20%) for L > 70 μm. For L < 70 μm, shapes are 50% bullet rosettes, 25% plates, and 25% hollow columns [*Baum et al.*, 2000].

[10] Correlations between *De* and *IWC* are improved by dividing the temperature in two groups, $-40 - -20$°C (warm cirrus) and $-65 - -40$°C (cold cirrus), as shown in Figure 1b. For warm cirrus, the correlation coefficients for parameterization are: a = 5.2375, b = 0.13142 and c = 0. For cold cirrus, we have a = 4.3257, b = 0.26535, and c = 0.021864. D_e for warm cirrus is generally larger than that for cold cirrus, and the range of *De* and *IWC* for midlatitude cirrus is narrower than that for the tropical counterpart.

[11] (c) In the Arctic region, our analysis is based on the in situ data collected during the DOE's ARM MPACE experiment at the ARM's North Slope of Alaska site in Fall 2004. Ice clouds were observed on only two days, October 17 and 18, consisting of a total of 1705 cases. But after data quality check, only 468 cases were used. These cases were largely from the UND Citation 2D-C measurements and the data points were averaged over 30 s to ensure adequate statistical sampling. For ice particles <100 μm, a Gamma distribution was used to extrapolate SDs to 2 μm based on the empirical coefficients derived by *Boudala et al.* [2002]. In terms of habit, *Korolev and Isaac* [1999] gave the percentage of pristine and irregular habits in different

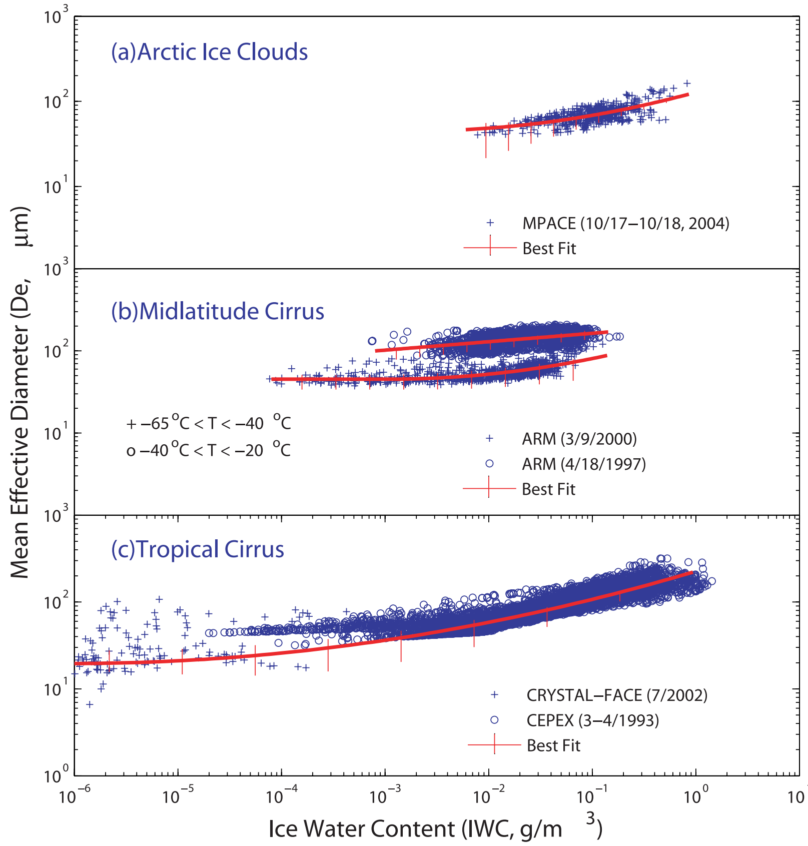

Figure 1. Mean correlation curves with uncertainties associated with small ice crystal concentration for *IWC* and *De* for (a) Arctic regions, (b) midlatitude, and (c) the tropics.

temperature bins for high latitude ice clouds. Because temperatures were much lower during MPACE observations, ice clouds are assumed to contain relatively more pristine particles (~ 20%) with the ratio of columns to plates of 100:20, as suggested by Korolev and Isaac, resulting in 3.3% plates and 16.7% columns. The remaining irregular ice particles include 40% bullet rosettes and 40% aggregates. The correlation coefficients for parameterization are: a = 4.8510, b = 0.33159 and c = 0.026189. *IWC* and *De* in Arctic ice clouds range from 10^{-2}–1 g/m^3 and from 50–120 μm, respectively. N_{sm} sensitivity experiments show that small particles contribute 5–20% as *IWC* increases, smaller than tropical and midlatitude cases. Arctic ice cloud *IWC* and *De* have narrower ranges than those in the other two regions. We were unable to find an obvious correlation between *De* and temperature, which ranges from −57 – −17°C for this dataset, possibly due to less stratification of the polar temperature profile.

3. Application to Radiation Calculations and General Circulation Models

[12] Broadband radiation flux calculations follow the approach developed by *Fu and Liou* [1992, 1993] and improved by *Gu et al.* [2003] for GCM applications. The solar and thermal IR spectra were divided into six and 12 bands, respectively, while the correlated k-distribution approach was used to sort the absorption lines for each band and overlap. In addition to the principal absorbing gases listed by *Fu and Liou* [1993] and *Gu et al.* [2003], we recently included absorption by water vapor continuum and a number of minor absorbers in the solar spectrum, including CH_4, N_2O, NO_2, O_3, CO, SO_2, O_2-O_2, and N_2-O_2. This led to an additional absorption of solar flux in a clear atmosphere on the order of 1–3 W/m^2 depending on the solar zenith angle and the amount of water vapor employed in the calculations.

[13] Input to the preceding radiative transfer program includes the optical depth τ, the single-scattering albedo ϖ_0, and the polynomial coefficients ϖ_i for phase function expansion in the context of the delta-four-stream approximation given by

$$\tau = IWP\left(a_0 + a_1/De + a_2/De^2\right),$$

$$1 - \varpi_0 = b_0 + b_1 De + b_2 De^2,$$

$$\varpi_i = c_{0i} + c_{1i} De + c_{2i} De^2, i = 1 - 4,$$

where *IWP* (ice water path) is the product of *IWC* and cloud thickness. The asymmetry factor $g = \varpi_1/3$ and a_n, b_n, and c_{ni} (n = 0–2) are fitting coefficients determined from the basic scattering and absorption database provided by *Yang et al.* [2000] for solar spectrum and *Yang et al.* [2005] for thermal IR spectrum. For solar bands, the first-order polynomial expansion is sufficient to achieve 0.1% accuracy. However,

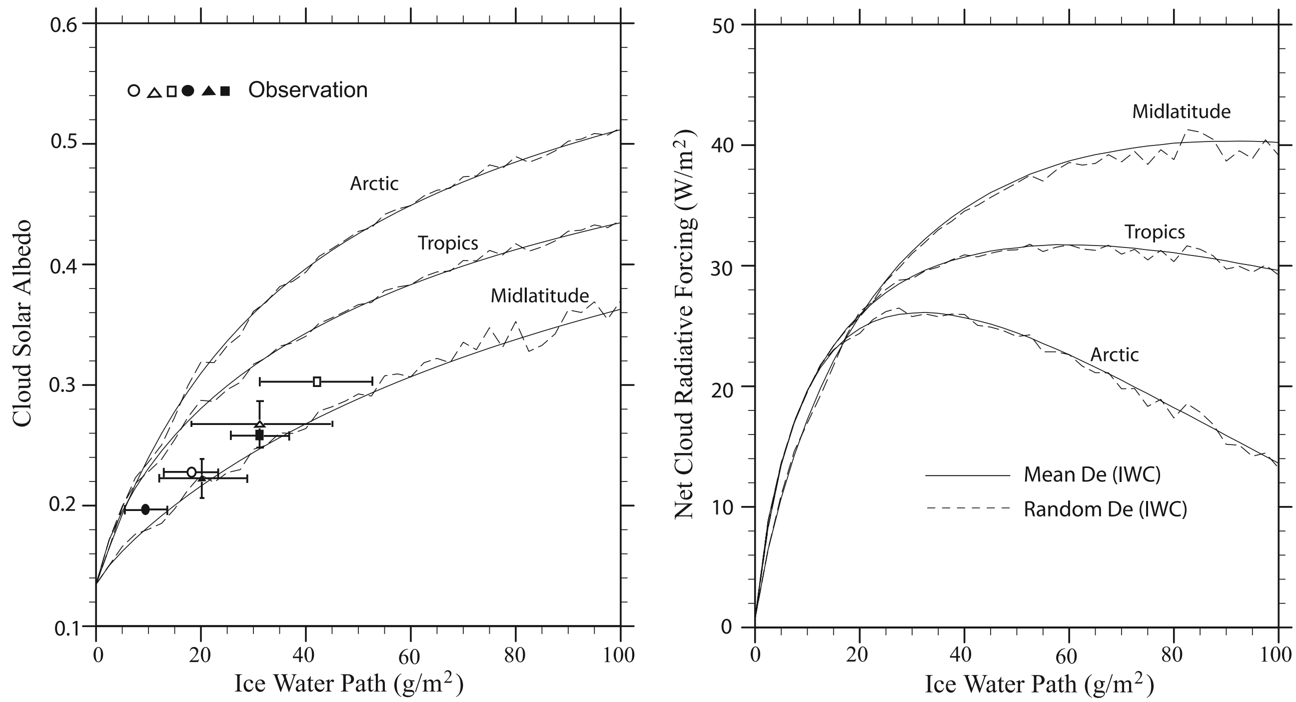

Figure 2. Solar albedo and net radiative forcing as a function of *IWP* for cirrus in the tropics, midlatitude, and Arctic. The solid lines correspond to the base run *IWC-De* curves denoted in Figure 1, while the fluctuated dashed curves are results computed from random numbers selected within the *De* deviations. Also shown in the solar albedo plot are observations for comparison purposes.

for thermal IR bands, the second-order polynomial fitting is required to achieve this level of accuracy.

[14] Figure 2 illustrates solar albedo and net radiative forcing as a function of *IWP* and *De*. The solar constant, solar zenith angle, surface albedo, cloud base height, and cloud thickness used in the calculations are 1366 W/m^2, 60°, 0.1, 9 km, and 2 km, respectively. For the same *IWP*, a cirrus cloud has the smallest *De* for the Arctic region and the largest for the warm midlatitude condition. It follows that the Arctic case displays the largest solar albedo and largest IR forcing (not shown), but the smallest net forcing because the negative solar radiative forcing increases more than the IR counterpart as *IWP* increases. Midlatitude results show the largest net forcing but smallest solar albedo associated with the largest *De*. For the same *IWC*, ice crystals can have different size distributions leading to different *De*. To account for *De* variation due to uncertainty in small ice crystal measurements, displayed are results calculated by using random *Des* that are within the possible range of the parameterized *De* related to this uncertainty corresponding to a specific *IWC* value as determined from observations. Differences in the solar albedo and net cloud radiative forcing produced by using the base run *De* and random values within uncertainty range associated with smaller ice crystal concentration are within about 5% or 2 W m^{-2}, revealing that using the *IWC-De* correlation in terms of mean would be an excellent approach for radiative forcing calculations. Also depicted are solar albedo observations presented by *Stackhouse and Stephens* [1991] in which the solar zenith angle was 61.3° and the surface albedo was estimated to be 0.072 during an intensive field experiment for cirrus clouds conducted in Wisconsin from 10/13–11/2, 1986. The observed data lies between the theoretical results representative of warm midlatitude and tropical regions.

[15] We incorporated the *IWC-De* correlation that accounts for uncertainty in small ice crystal measurements in the UCLA GCM to investigate its usefulness and importance in climate simulations. Two numerical experiments were carried out. In the control run, *De* for ice clouds was fixed at 80 μm. In the perturbation run, *De* is parameterized in terms of *IWC* in accordance with the correlation equations presented above. It is a function of the model predicted *IWC* at each time-step and interacts with cloud, radiation and dynamic processes in the model. *De*s from parameterization are generally smaller in the tropics than in the midlatitude, ranging from 20 to 80 μm. In the midlatitude, *De* ranges from 30 to ~50 μm for colder temperature ($-65°C < T < -40°C$), and 70 to > 100 μm for warmer cirrus. In the Arctic region, *De* is ~ 50–70 μm.

[16] The geographical distributions of differences between OLR and precipitation are illustrated in Figure 3. Since smaller ice particles reflect greater solar radiation and trap more IR, differences in OLR closely follow variation in *De*. Negative values are mostly located in lower latitudes and a portion of higher latitudes where the parameterized *De*s are generally smaller than the prescribed value in the control run, resulting in more trapped IR fluxes. Increased OLRs are found in some midlatitude regions due to larger *De* than the prescribed 80 μm. Differences between the two simulations are less significant in high latitudes since the parameterized *De* is closer to a fixed value of 80 μm in the

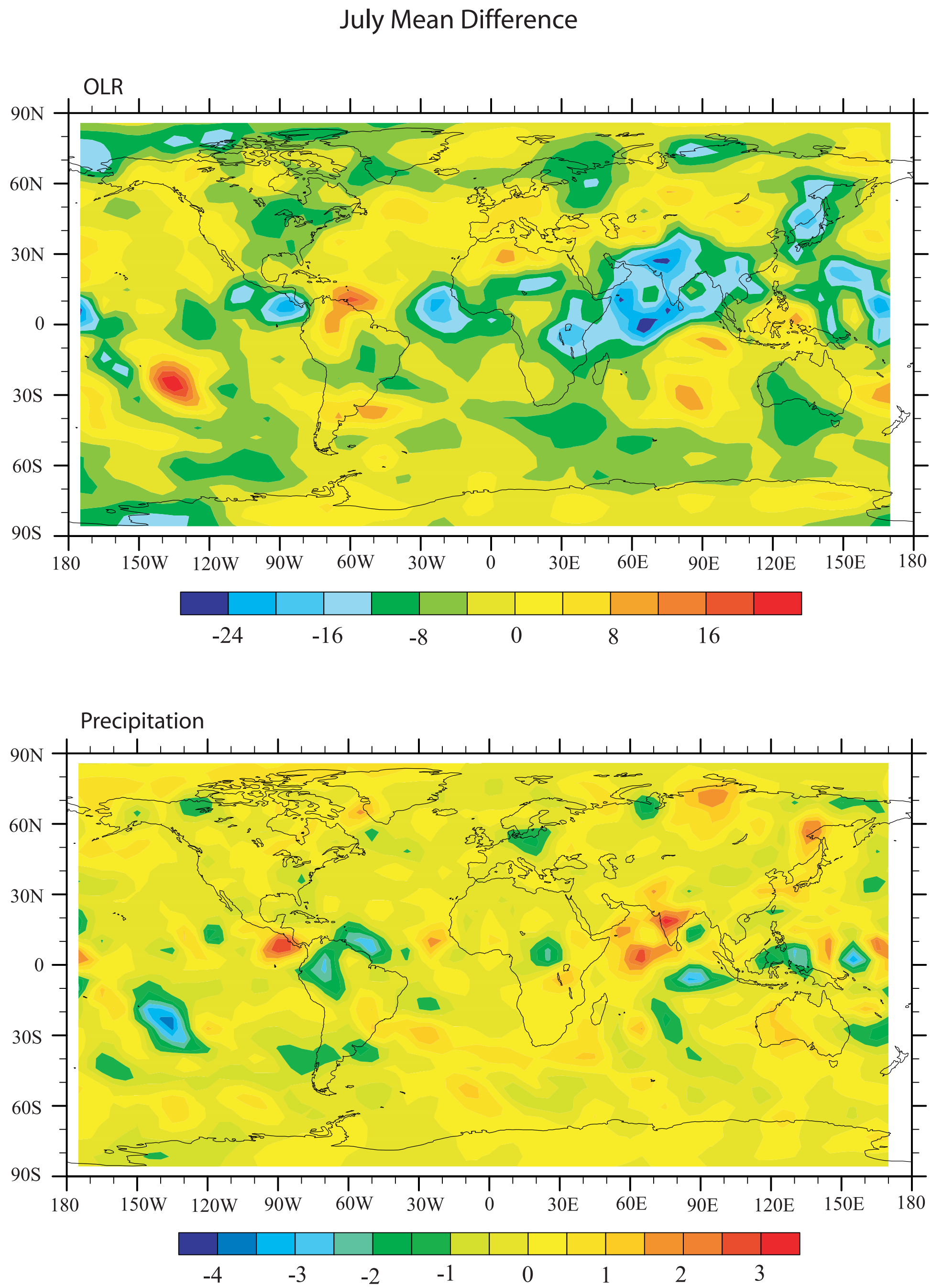

Figure 3. July mean differences in the OLR (w/m^2) and precipitation (mm/day) patterns between UCLA GCM simulations based on *Des* determined from the *IWC*-*De* correlations for the three regions and the control run using a fixed ice crystal size.

control run. Also, OLR increases more in the southern hemisphere associated with less cloudy areas simulated from the UCLA GCM. Changes in the precipitation pattern are not direct results of the *De* effect, but are related to intricate interactions among cloud, radiation, and dynamic processes through the modified vertical heating profiles associated with the interactive *De* used in the simulation. Increases in precipitation are mostly located in tropical regions where OLRs are reduced, an indication of stronger convective activities. Reduced precipitation is found in areas corresponding to enhanced OLRs in subtropical and midlatitude regions. This brief illustration suffices to demonstrate the importance of using correct ice *De*s in GCM simulations.

4. Concluding Remarks

[17] Correlation analysis between *IWC* and *De* has been carried out using a large set of observed ice crystal size distributions obtained from a number of cirrus field campaigns in the tropics, midlatitude, and Arctic. From fundamental microphysics analysis, *IWC* and *De* are directly related through their physical definitions. We showed that *IWC* and *De* are well-correlated using this regional division

and found that correlations between *De* and temperature for tropical cirrus and Arctic ice clouds are relatively insignificant. Including temperature classification in midlatitude cases, however, increases *De-IWC* correlation. Tropical cirrus *IWC* spans a wide range, 10^{-6}–1 g/m^3, with corresponding *De* values spanning from 20 to 200 μm. Midlatitude cirrus have ranges of 10^{-4}–10^{-1} g/m^3 for *IWC* and 30–140 μm for *De*, while Arctic ice clouds have the narrowest *IWC* (10^{-2}–1 g/m^3) with a *De* range of 50–120 μm.

[18] Using the *IWC-De* correlation for the three geographical regions, we performed calculations for cloud radiative forcing parameters as a function of *IWP* in which *Des* (*IWCs*) are given as mean and deviation of the correlation. Uncertainty in small ice crystal measurements in the correlation leads to deviations from the mean by less than 2 W/m^2 in radiative forcing values, revealing *De* is an excellent parameter for radiation calculations. The largest solar radiative forcing occurs in the Arctic region, but with the lowest net radiative forcing from about a few to 25 W/m^2. Using the correlation results, UCLA GCM simulations showed substantial regional deviations in OLR and precipitation patterns from assuming a constant *De*. *De* and *IWC*, two independent parameters physically connected through ice crystal size distribution, are basic units to drive radiation calculations. We used the observed ice crystal size distributions in representative geographic regions to constrain *De* through *IWC* without the necessity of incorporating intricate ice microphysics in GCMs. Finally, we argue that temperature is not an ideal parameter for *De* parameterization in climate models on the basis of theory and observation. However, it can be used to increase correlation parameterization for midlatitude cirrus clouds.

[19] **Acknowledgments.** This work has been supported by DOE grant DE-FG03-00ER62904 and NSF grant ATM-0331550. We thank D. Baumgardner and J. Mace for assistance in this research.

References

Baum, B. A., P. F. Soulen, K. I. Strabala, M. D. King, S. A. Ackerman, W. P. Menzel, and P. Yang (2000), Remote sensing of cloud properties using MODIS airborne simulator imagery during SUCCESS: 2. Cloud thermodynamic phase, *J. Geophys. Res.*, *105*, 11,781–11,792.

Boudala, F., et al. (2002), Parameterization of effective ice particle size for high-latitude clouds, *Int. J. Climatol.*, *22*, 1267–1284.

Fu, Q., and K. N. Liou (1992), On the correlated k-distribution method for radiative transfer in nonhomogeneous atmospheres, *J. Atmos. Sci.*, *49*, 2139–2156.

Fu, Q., and K. N. Liou (1993), Parameterization of the radiative properties of cirrus clouds, *J. Atmos. Sci.*, *50*, 2008–2025.

Gu, Y., and K. N. Liou (2006), Cirrus cloud horizontal and vertical inhomogeneity effects in a GCM, *Meterorol. Atmos. Phys.*, *91*, 223–235.

Gu, Y., J. Farrara, K. N. Liou, and C. R. Mechoso (2003), Parameterization of cloud-radiation processes in the UCLA general circulation model, *J. Clim.*, *16*, 3357–3370.

Heymsfield, A., and G. McFarquhar (1996), High albedos of cirrus in the tropical Pacific warm pool, *J. Atmos. Sci.*, *53*, 2424–2451.

Heymsfield, A., and M. Platt (1984), A parameterization of the particle size spectrum of ice clouds in terms of the ambient temperature and the ice water content, *J. Atmos. Sci.*, *41*, 846–856.

Heymsfield, A., et al. (2006), Effective radius of ice particle populations derived from aircraft probes, *J. Atmos. Oceanic Technol.*, *23*, 361–380.

Ivanova, D., D. Mitchell, W. Arnott, and M. Poellot (2001), A GCM parameterization for bimodal size spectra and ice mass removal rates in midlatitude cirrus clouds, *Atmos. Res.*, *59–60*, 89–113.

Korolev, A., and G. Isaac (1999), Ice particle habits in Arctic clouds, *Geophys. Res. Lett.*, *26*, 1299–1302.

Kristjánsson, J. E., T. Iversen, A. Kirkevåg, Ø. Seland, and J. Debernard (2005), Response of the climate system to aerosol direct and indirect forcing: Role of cloud feedbacks, *J. Geophys. Res.*, *110*, D24206, doi:10.1029/2005JD006299.

Liou, K. N., and S. Ou (1989), The role of cloud microphysical processes in climate: An assessment from a one-dimensional perspective, *J. Geophys. Res.*, *94*, 8599–8607.

McFarquhar, G., and A. Heymsfield (1997), Parameterization of tropical cirrus ice crystal size distributions and implications for radiative transfer: Results from CEPEX, *J. Atmos. Sci.*, *54*, 2187–2200.

McFarquhar, G., S. Iacobellis, and R. Sommerville (2003), SCM simulations of tropical ice clouds using observationally based parameterizations of microphysics, *J. Clim.*, *16*, 1643–1664.

Ou, S., and K. N. Liou (1995), Ice microphysics and climatic temperature perturbations, *Atmos. Res.*, *35*, 127–138.

Ou, S., et al. (1995), Remote sounding of cirrus cloud optical depths and ice crystal sizes from AVHRR data: Verification using FIRE-II-IFO measurements, *J. Atmos. Sci.*, *52*, 4143–4158.

Stackhouse, P., and G. Stephens (1991), A theoretical and observational study of the radiative properties of cirrus: Results from FIRE 1986, *J. Atmos. Sci.*, *48*, 2044–2059.

Twomey, S., M. Piepgrass, and T. Wolfe (1984), An assessment of the impact of pollution on global cloud albedo, *Tellus, Ser. B*, *36*(1984), 356–366.

Yang, P., K. N. Liou, K. Wyser, and D. Mitchell (2000), Parameterization of the scattering and absorption properties of individual ice crystals, *J. Geophys. Res.*, *105*, 4699–4718.

Yang, P., et al. (2005), Scattering and absorption property database for nonspherical ice particles in the near- through far-infrared spectral region, *Appl. Opt.*, *44*, 5512–5523.

Yue, Q., et al. (2007), Interpretation of AIRS data in thin cirrus atmospheres based on a fast radiative transfer model, *J. Atmos. Sci.*, *64*, 3827–3842.

Y. Gu, K. N. Liou, and Q. Yue, Department of Atmospheric and Oceanic Sciences and Joint Institute for Regional Earth System Science and Engineering, University of California, Los Angeles, CA 90095, USA.

G. McFarguhar, Department of Atmospheric Sciences, University of Illinois, Urbana, IL 61801, USA.